Journal of Catalysis **193,** 80–87 (2000)
doi:10.1006/jcat.2000.2877, available online at http://www.idealibrary.com on IDEAL®

Synthesis of Ammonia at Atmospheric Pressure with the Use of Solid State Proton Conductors

George Marnellos, Stergios Zisekas, and Michael Stoukides[1]

Chemical Engineering Department and Chemical Process Engineering Research Institute, University Campus, University Box 1517, Thessaloniki 54006, Greece

Received November 8, 1999; revised March 22, 2000; accepted March 24, 2000

Ammonia was synthesized from nitrogen and hydrogen at atmospheric pressure in a solid state proton-conducting cell reactor. Two types of reactors were used, one double-chamber and one single-chamber cell. In the double-chamber cell, hydrogen flowed over the anode and was converted into protons that were transported through the solid electrolyte and reached the cathode (Pd) over which nitrogen was passing. At 570°C, nearly 80% of the electrochemically supplied hydrogen was converted into ammonia. In the single-chamber cell, hydrogen and nitrogen were fed in together and the solid electrolyte cell was suspended in the gaseous stream. At 750°C, a NEMCA effect was observed but the enhancement was not very strong ($\Lambda < 2$). This novel process eliminates the thermodynamic requirements on the temperature and pressure of operation of conventional catalytic reactors. © 2000 Academic Press

Key Words: **ammonia synthesis; solid state proton conductors; palladium electrodes.**

INTRODUCTION

The dominant process for ammonia synthesis (Haber process) was developed at the beginning of the twentieth century and involves the reaction of gaseous nitrogen and hydrogen on a Fe-based catalyst at high pressures (150–300 bar)

$$N_2 + 3H_2 <----> 2NH_3. \quad [1]$$

The conversion to ammonia is limited by thermodynamics. The gas volume decreases with reaction. Hence, very high pressures must be used in order to push equilibrium to the right. Also, the reaction is exothermic and therefore conversion increases with decreasing temperature. However, in order to achieve industrially acceptable reaction rates, the reaction temperature must be high.

In the early stages of the development of the Haber process, pressures in the 500–1000 bar range were used (1–3). The continuous search for more active catalysts made it possible to operate at lower temperatures and consequently at lower pressures as well. Currently, the operating pressure for most modern synthesis loops falls in the 100–300 bar pressure range and in the 450–500°C range at which the equilibrium conversion is of the order of 10–15% (1, 2).

It is beyond the purpose of this communication to review the research that has been conducted thus far concerning the kinetics and the mechanism of ammonia synthesis. Numerous works have been reported in literature and fortunately, several informative and comprehensive reviews have been published from time to time (4–7).

In the present communication, an alternative route to ammonia synthesis at atmospheric pressure is presented. Solid state proton (H^+) conductors are used and hydrogen is supplied electrochemically. A model process using solid state proton conductors to obtain conversions higher than those predicted by the reaction equilibrium, has been proposed in the past (8, 9). The principle is as follows. Gaseous H_2 passing over the anode of the cell reactor, will be converted to H^+:

$$3H_2 ----> 6H^+ + 6e^-. \quad [2]$$

The protons (H^+) are transported through the solid electrolyte to the cathode where the half-cell reaction

$$N_2 + 6H^+ + 6e^- ----> 2NH_3 \quad [3]$$

takes place. Thus, reaction [1] is again the overall reaction.

Preliminary experimental verification of these model predictions has already been presented (10). The present communication contains results obtained with both a regular double-chamber and a single-chamber cell reactor.

EXPERIMENTAL METHODS

The experimental apparatus employed for the catalytic and electrocatalytic measurements consisted of the feed unit, the cell reactor and the analysis system. The reactants, N_2 and H_2 and the diluent He were of 99.99% purity. Schematic diagrams of the two cell-reactors are shown in Figs. 1 and 2, respectively. The reactor of Fig. 1 consisted of a

[1] To whom correspondence should be addressed.

0021-9517/00 $35.00

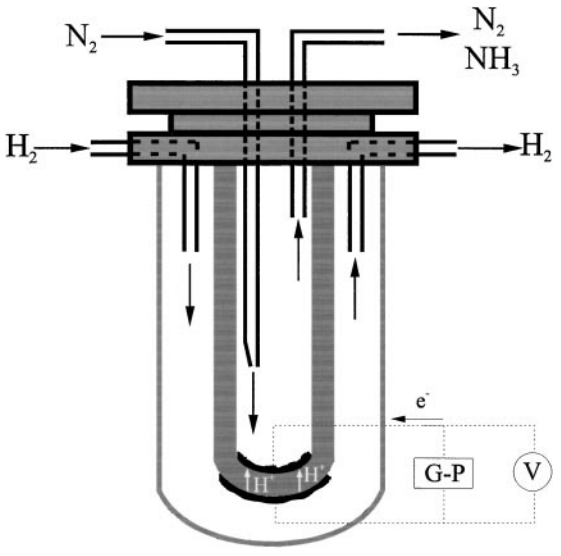

FIG. 1. Schematic diagram of the double-chamber reactor cell.

nonporous ceramic tube (18 cm long, 1.25 cm inside diameter, and 1.55 cm outside diameter) closed at the bottom end. The ceramic material was a strontia–ceria–ytterbia (SCY) perovskite of the form $SrCe_{0.95}Yb_{0.05}O_3$. The ceramic tube was enclosed in a quartz tube. Two porous polycrystalline palladium films were deposited on the inside and outside walls of the SCY tube and served as cathodic and anodic electrodes, respectively.

The single-chamber cell reactor is presented schematically in Fig. 2. The SCY disk (1–2 mm thickness and 1.9 cm diameter) was suspended into a quartz tube (18 cm long, 2.75 cm inside diameter and 3.16 cm outside diameter). The two palladium films (cathode and anode) were prepared from a palladium paste (Engelhard, A2985) and deposited on the two sides of the disk. The electrodes were then calcined at 800°C for 2 h. Scanning electron micrographs of the Pd electrode showed that the average diameter of the crystallites was approximately 2 μm. The catalyst loading used for preparation of the cathodic electrode was 32 mg of Pd for the double chamber and 24 mg for the single chamber. Using the above crystallite size, a total catalyst surface area of 80 cm^2 for the double and 60 cm^2 for the single-chamber cell reactor was estimated. The superficial surface area of each electrode was 1.3 and 1 cm^2 for the double- and single-chamber reactor configurations, respectively. Details on the catalyst preparation, construction of the cell reactors, and analysis of reactants and products can be also found in previous communications (10, 11).

Analysis of the inlet and outlet gas was performed by on-line gas chromatography with a molecular sieve 13X and a porapak N columns. The consumption of nitrogen (inlet minus outlet) was also measured on-line. In addition to the GC measurements, the gaseous outlet stream was bubbled for about 1 h through a flask that contained 75 ml of HCl with initial pH about 4.00. An electronic pH meter was used to measure the pH before and after passing the gas through the flask. The difference in pH, converted into reacted HCl, was in very good agreement with the amount of NH_3 produced according to the GC measurements. Also, "blank" tests were done by bubbling the exit gas for 1 h through the flask with the cell operating under open circuit ($I = 0$). There was no pH change in the blank tests. Finally, in several occasions, samples from the titration flasks were checked for ammonia content by using Nessler's reagent. The results were positive for the "closed-circuit" samples and negative for the "blank" samples.

The electrochemical properties of perovskites depend strongly on their chemical composition. Proton transference numbers (t_{H+}) reported in the literature for SCY vary considerably (12–15). This is because the t_{H+} of the SCY depends not only on temperature but also on the composition of the gas to which the electrolyte surface is exposed and on the imposed current density. It has been observed that SCY is a pure H^+ conductor when exposed to H_2 on one side and Ar on the other, but becomes a mixed conductor when O_2 is cofed with Ar (13). The results of Hamakawa *et al.* (13) and Chiang *et al.* (14), however, showed that at the conditions employed in the present work ($T = 550$–750°C, $I < 2$ mA/cm^2, He–N_2 mixtures) the t_{H+} must be very close to unity. It should also be mentioned that the proton transference number was measured in the double-chamber cell by passing 100% H_2 from the anode and 100% He from the cathode. The amount of hydrogen evolved at the cathode was compared to $I/2F$ (=moles H_2/s transported through

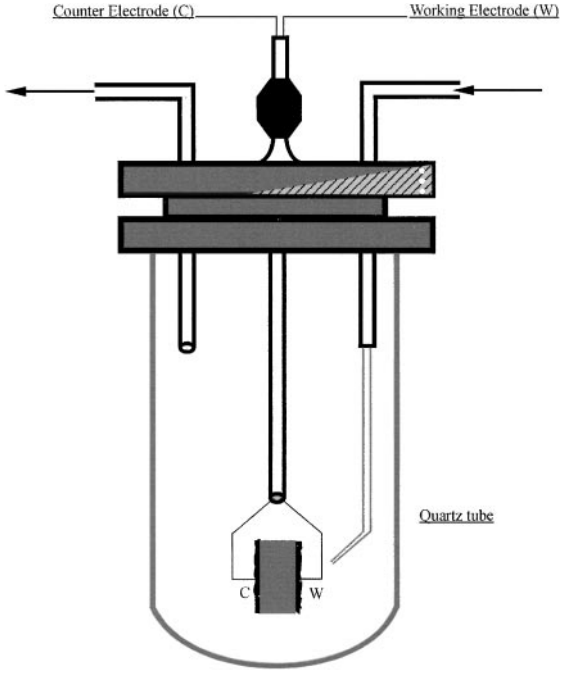

FIG. 2. Schematic diagram of the single-chamber reactor cell.

the electrolyte) and they were found to be within $\pm 5\%$ equal to each other.

One of the applications of H^+ conductors is the operation of either the double-chamber cell (Fig. 1) or of the single-chamber cell (Fig. 2) as an ionic (protonic) pump (16). An external power source is used to direct and control the current. According to Faraday's law, the current I corresponds to a molar flux of $I/2F$ moles of H_2/s. The change in the rate of hydrogen consumption at the cathode can be compared to $I/2F$, the rate of electrochemical flux of hydrogen through the solid electrolyte. The dimensionless rate enhancement factor Λ is defined (17, 18) as

$$\Lambda = \Delta r/(I/2F), \qquad [4]$$

where Δr is the increase in the catalytic rate of hydrogen consumption (in moles per second). In studies in which the total amount of hydrogen required for the reaction is supplied electrochemically as H^+, the maximum attainable rate of hydrogen consumption at the cathode is equal to the rate of H^+ transport through the solid electrolyte, i.e., $\Lambda = 1$. This is the case of *Faradaic* operation. If, however, gaseous H_2 is cofed with the reactant in the gas phase, then it would be possible for Λ to exceed unity. A value of Λ equal to 10^2 means that for each mole of hydrogen pumped through the electrolyte, 100 moles of additional gaseous hydrogen react. This is the case of *non-Faradaic* operation. This phenomenon of non-Faradaic Electrochemical Modification of Catalytic Activity, named NEMCA, has been attributed to changes in the catalyst work function caused by ionic pumping (17, 18). Since the first study in which this non-Faradaic enhancement of reaction rate was observed (19) and in which the values of Λ were of the order of 100, numerous catalytic systems have been studied and Λ values as high as 3×10^5 have been reported (18). Today, it is well established (17, 18) that the NEMCA phenomenon is due to electrochemically imposed spillover of ions from the solid electrolyte to the electrode–catalyst surface and it is these ions that act as promoters for the catalytic reactions.

RESULTS

The experimental results obtained with the double- and single-chamber cell reactor are presented separately starting with those of the double-chamber cell reactor. It should be pointed out that the data of Fig. 3 have already been presented in a previous publication (10) but are presented again in order to facilitate the understanding for the readers.

a. Double Chamber Cell Reactor

The rate of NH_3 formation is shown in Fig. 3 as a function of $I/2F$. Under the experimental conditions of the present study, the proton transference number (t_{H+}) is very close

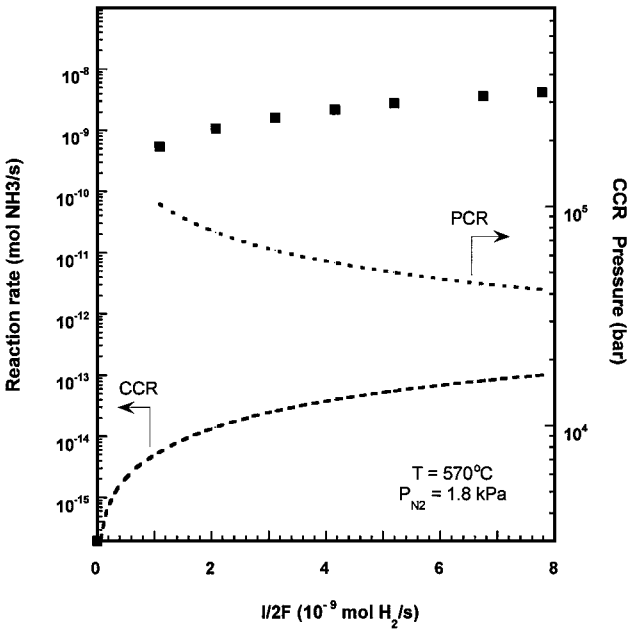

FIG. 3. Dependence of the ammonia production rate on the H^+ pumping rate, $I/2F$ (double-chamber cell, $T = 570°C$, $P_{N2} = 1.8$ kPa).

to unity and therefore, the ratio $I/2F$ is equal to the electrochemical molar flux of hydrogen through the solid electrolyte. The cell of Fig. 1 was kept at 570°C. A mixture of 1.8% N_2 in He was passed over the cathode at a volumetric rate of 8.3×10^{-8} m^3/s and at atmospheric total pressure. A flow of 5.0×10^{-7} m^3/s of 100% hydrogen at atmospheric pressure was maintained over the anode. At $I = 0$, no products were formed. Upon imposing a current through the cell, NH_3 appeared at the cathode and, after a transient period of 2 to 6 min, a steady-state rate of NH_3 formation was established.

The two dotted lines in Fig. 3 are based on thermodynamic calculations and compare the present results with those that would have been obtained in a conventional catalytic reactor (CCR) in which the inlet molar flowrate of gaseous H_2 is equal to $I/2F$. The CCR curve compares the present cell reactor with a hypothetical catalytic reactor (CCR). In the CCR, all the reactants are gases, the inlet molar flowrates of nitrogen and helium are the same as in the cell reactor, and the inlet molar flowrate of gaseous hydrogen is equal to $I/2F$. It is further assumed that in the CCR, the residence time is so long and the catalyst so effective that the exit molar flowrate of ammonia corresponds to thermodynamic equilibrium of reaction [1] at 570°C and atmospheric pressure. Hence, the CCR curve represents the maximum rate of NH_3 production that can be obtained in a conventional reactor. It can be seen that the NH_3 production rates attained in the present experiments exceed the CCR rates by at least three orders of magnitude. The PCR curve, scaled on the right-hand side vertical axis of Fig. 3, does not represent reaction rates, it represents a pressure.

It is the pressure at which the CCR should operate in order for the ammonia production rate to be equal to that obtained in the present cell reactor. Stating it differently, the PCR curve shows the minimum pressure of operation of a CCR that gives the same NH_3 formation rate as the cell reactor. It can be seen that the calculated pressure values are of the order of 10^4 bar.

In the experiments of Fig. 3, the electrochemically supplied H_2 was almost completely converted into NH_3. The corresponding conversion for N_2 was considerably lower. This difference, however, cannot be attributed to low reactivity of N_2. In these experiments, hydrogen was the limiting reactant and therefore, the rates of ammonia formation were very close to two-thirds the rates of hydrogen supply, according to the stoichiometry of reaction [1].

The reactor of Fig. 1 was also used to study the effect of the partial pressure of N_2 on the rate of NH_3 formation. Experiments were done at 570°C for three different partial pressures (P_{N2}) of nitrogen, 0.003, 0.01, and 0.018 bar. Again, only nitrogen (no hydrogen) diluted in helium was flowing over the cathode while the anode was exposed to a 100% H_2 stream. It was found that the reaction rate was essentially independent of the partial pressure of nitrogen (10).

Ammonia decomposition at the temperatures of the present experiments can be significant both on the catalyst surface and in the gas phase. In order to diminish the rate of NH_3 decomposition, the double-chamber reactor cell was designed in such a way that only the bottom of the SCY tube was at the operating temperature, whereas most of the tube was placed outside the furnace. The degree of NH_3 decomposition at 570°C was quantitatively determined from open circuit ($I = 0$) experiments in which gaseous NH_3 was introduced together with N_2 and He at flow rates similar to those employed in the NH_3 synthesis experiments. The percent ammonia decomposition was found to vary between 15 and 30%. Furthermore, the reaction of NH_3 decomposition was studied under closed circuit in order to examine the effect of electrochemical H^+ pumping on the reaction rate. The double-chamber cell of Fig. 1 was used in these experiments and the temperature was kept at 570°C. A gaseous mixture of 0.13% NH_3, 0.135% N_2 (balance He) was introduced over the cathode at atmospheric total pressure. The anode was exposed to a 100% H_2 stream. At open circuit, about 25% of ammonia decomposed, which corresponded to a steady-state rate of NH_3 decomposition of 8.2×10^{-9} mole/s. Figure 4 shows the effect of H^+ pumping to the cathode surface. The decomposition rate decreases almost linearly with $I/2F$ to reach a value of 4.5×10^{-9} mole/s, which corresponds to a 15% decomposition.

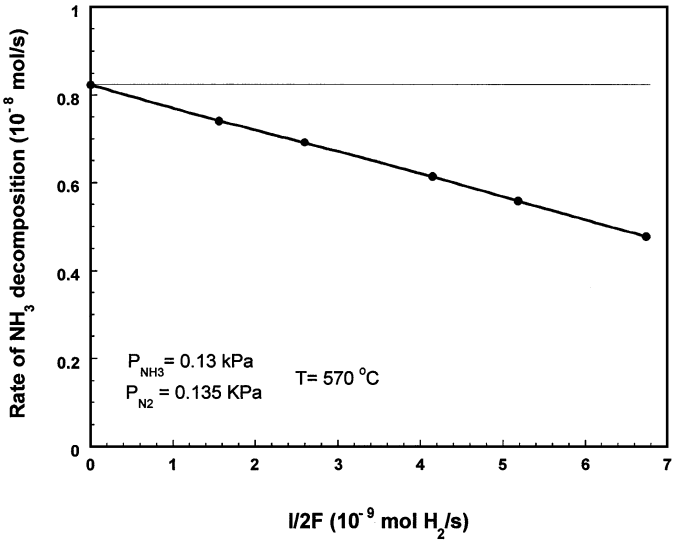

FIG. 4. Dependence of the ammonia decomposition rate on the H^+ pumping rate, $I/2F$ (double-chamber cell, $T = 570$°C, $P_{NH3} = 0.13$ kPa, $P_{N2} = 0.135$ kPa).

b. Single-Chamber Cell Reactor

Figure 5 contains results obtained in the single-chamber cell reactor of Fig. 2. The cell was kept at a temperature of 750°C. A stoichiometric mixture of hydrogen and nitrogen was introduced into the reactor (2% nitrogen, 6% hydrogen) and helium was used again as diluent. Figure 5a shows that the rate of ammonia formation increases by increasing the current imposed to the cell, i.e., by increasing the electrochemical hydrogen pumping rate from the counter to the working electrode. The ammonia rates experimentally achieved are higher than the corresponding CCR rates by at least two orders of magnitude. Again, as denoted by the PCR curve, the total pressure at which a conventional catalytic reactor should operate in order to attain the current ammonia production rates is very high (of the order of 10^3 bar).

Figure 5b shows the dependence of the percent conversions of H_2 and N_2 on the rate of hydrogen electrochemical supply, $I/2F$. The bottom dotted line corresponds to the maximum (equilibrium) hydrogen or nitrogen conversion that could be attained in a CCR. Similar to the case of the double-chamber reactor cell, the conversions achieved under closed circuit are much higher (two to three orders of magnitude) than those attainable in a conventional catalytic reactor. The difference here is that the nitrogen and hydrogen conversions are equal to each other and this is expected because stoichiometric mixtures of these gases were introduced. Figure 5c shows the Λ values obtained in these experiments. Although Λ exceeds unity, it does not attain impressively high values. It is generally between 1 and 2. So, the NEMCA effect is observed but the Λ values are not very far from unity.

Figure 6a shows the effect of P_{H2}/P_{N2}, the feed gas phase ratio of H_2 to N_2, on the rate of ammonia formation. The rate of electrochemical hydrogen transport was kept

constant at 5.18×10^{-9} mole/s (or equivalently constant current $I = 1$ mA) and the temperature was kept at 750°C. Clearly, the reaction rate increases with increasing P_{H2}/P_{N2}. The corresponding Λ values are shown in Fig. 6b.

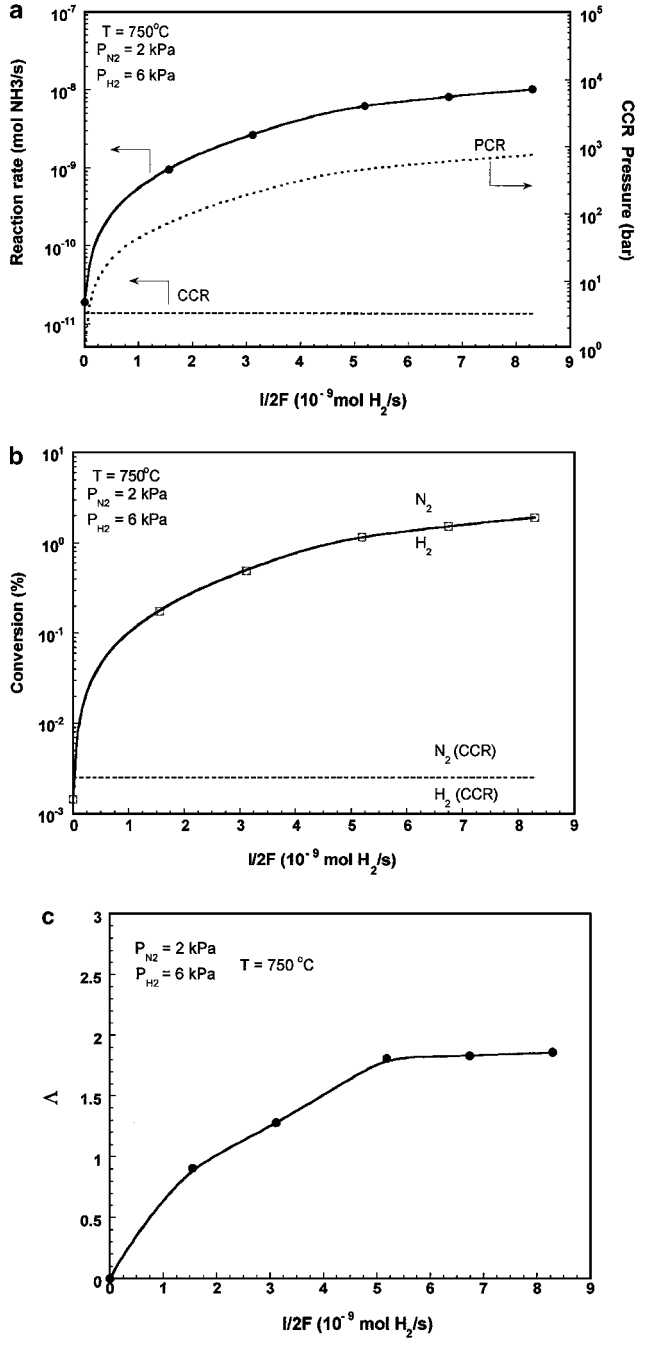

FIG. 5. (a) Dependence of the ammonia production rate on the H^+ pumping rate, $I/2F$ (single-chamber cell, $T = 750°C$, $P_{N2} = 2$ kPa, $P_{H2} = 6$ kPa). (b) Dependence of the hydrogen and nitrogen conversion on the H^+ pumping rate, $I/2F$ (single-chamber cell, $T = 750°C$, $P_{N2} = 2$ kPa, $P_{H2} = 6$ kPa). (c) Dependence of the enhancement factor Λ on the H^+ pumping rate, $I/2F$ (single-chamber cell, $T = 750°C$, $P_{N2} = 2$ kPa, $P_{H2} = 6$ kPa).

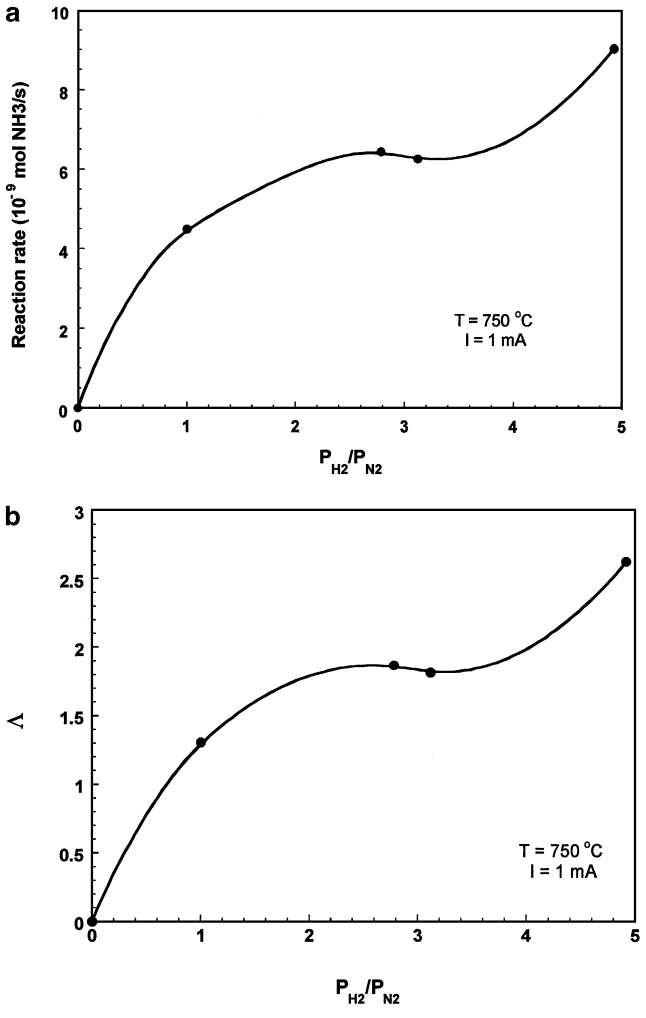

FIG. 6. (a) Effect of the partial pressures ratio, P_{H2}/P_{N2}, on the ammonia production rate, r_{NH3} (single-chamber cell, $T = 750°C$, $I = 1$ mA). (b) Effect of the partial pressures ratio, P_{H2}/P_{N2}, on the electrochemical enhancement factor Λ (single-chamber cell, $T = 750°C$, $I = 1$ mA).

DISCUSSION

It is relatively well established that in the typical catalytic system for ammonia synthesis (Fe-based catalyst, pressures of the order of 100 bar, 450–500°C), the rate-determining step is the dissociative adsorption of the gaseous molecular nitrogen onto the catalyst's active sites (1, 4). The reaction conditions in the present work were quite different: Pd catalyst, atmospheric pressure, temperatures between 570 and 750°C, and most important, the reactant hydrogen was supplied electrochemically either partly (in the single-chamber reactor) or wholly (in the double-chamber reactor). Hence, it is reasonable to expect either the reaction mechanism to be different or at least the rate-determining step to be different.

In the double-chamber experiments, the reaction rate was limited by the rate of proton transport through the

electrolyte. It was found that a sixfold increase in P_{N2} has an insignificant effect on the rate of ammonia synthesis (10). To study intrinsic kinetics, one should decrease the ohmic resistance of the solid electrolyte so that the flux of H^+ increases. This, however, would require operation at much higher temperatures where the undesirable reaction of ammonia decomposition would increase considerably. The decomposition results showed that under the conditions of the double-chamber experiments, 20% or less of the ammonia fed in the reactor decomposed into its elements. These results, combined with those of Fig. 3 in which at least 75% of the electrochemically transported hydrogen was converted into ammonia, indicate that the initial conversion of H^+ into NH_3 may be complete and the unreacted hydrogen found at the cathode comes from the subsequent gas phase decomposition of NH_3. This is also quantitatively justified by the data of Fig. 4. From the values of $I/2F$, one can calculate the maximum amount of NH_3 that can be formed ($=2/3 \times I/2F$). The difference between the rate of NH_3 decomposition under open circuit (horizontal line in Fig. 4) and under closed circuit (line through data points in Fig. 4) is very close to 80% of $2/3 \times I/2F$. This is a strong indication that the electrochemically transported hydrogen is first completely converted into ammonia and afterward about 20–25% of this ammonia decomposes either on the catalyst or in the gas phase.

The single-chamber results, which are summarized in Figs. 5 and 6, can provide additional information on the reaction pathway since the catalyst–electrode surface was exposed to both reactant gases, H_2 and N_2. In the present experiments, the non-Faradaic enhancement parameter Λ was found to vary between 1.0 and 2.0, which indicates that the Pd surface is electrochemically modified to a moderate extent (weak NEMCA effect). Nevertheless, values of Λ exceeding unity indicate that it is not necessary for all hydrogen required for the formation of ammonia to be supplied electrochemically. If the effect was solely electrocatalytic (Faradaic), the values of Λ would be less or equal to 1.0. Hence, in these experiments, a non-Faradaic enhancement is observed although the effect of catalyst modification is rather weak.

The NEMCA effect is due to the spillover of ions which originate from the solid electrolyte and migrate on the metal (electrode) surface (17, 18). These spillover ions (protons in the present case) with their compensating charges spread on the metal, form dipoles which alter the catalyst work function and consequently the catalytic properties (17). There are no previous NEMCA studies of this reaction reported in the literature. The closest related NEMCA study can be considered that of NH_3 decomposition on Fe in which H^+ and K^+ solid state conductors were used (20). In that study, the rate of NH_3 decomposition was found to decrease significantly upon decreasing the catalyst potential, i.e., upon supplying H^+ or K^+ to the catalyst surface. The effect of K^+ was more pronounced leading to an almost complete poisoning of the reaction (20). The explanation of these results was that by decreasing the catalyst potential and therefore decreasing the catalyst work function, the binding strength of electron acceptor adsorbates, such as N, was increased while the binding strength of electron donor adsorbates, such as NH_3 and H, was decreased (20).

The same interpretation could hold for the present results of Figs. 5 and 6. By "pumping" H^+ ions to the Pd surface, the catalyst work function decreases and consequently, the N–Pd bond is strengthened and stabilized. At the same time, the Pd–NH_3 and Pd–H bonds are weakened. This could also explain the behavior pictured in Fig. 6, where by increasing the P_{H2}/P_{N2} ratio, both reaction rate and electrochemical enhancement factor (Λ) increase. By imposing a constant flux of protons from the solid electrolyte to the cathode, the catalytic properties are modified to such an extent that the effect of P_{H2} becomes much more pronounced than that of P_{N2}.

Nevertheless, the interpretation of the present results can be quite different. In a very recent publication, Rod *et al.* (21) used density functional calculations to compare the biological and the industrial catalytic synthesis of ammonia. Their calculations suggest that in the biological process, N_2 is hydrogenated to ammonia without dissociation. The requirement for this pathway to be successful is the availability of protons. Therefore, it is possible the reaction pathway of the present electrochemical process is the same as that of the biological process.

As already mentioned, a very weak NEMCA effect was observed in this study (Λ values between 1 and 2). There is a thermodynamic rather than kinetic explanation for these low Λ values. Assuming isothermal operation of the cell, one can write steady-state energy and entropy balances for the single-chamber cell reactor:

$$\begin{aligned}\Delta H = {} & n_{\mathrm{He,out}}H_{\mathrm{He,out}} + n_{\mathrm{H2,out}}H_{\mathrm{H2,out}} + n_{\mathrm{N2,out}}H_{\mathrm{N2,out}} \\ & + n_{\mathrm{NH3,out}}H_{\mathrm{NH3,out}} - n_{\mathrm{H2,in}}H_{\mathrm{H2,in}} - n_{\mathrm{N2,in}}H_{\mathrm{N2,in}} \\ & - n_{\mathrm{He,in}}H_{\mathrm{He,in}} = Q' - P \qquad [5]\end{aligned}$$

$$\begin{aligned}\Delta S = {} & n_{\mathrm{He,out}}S_{\mathrm{He,out}} + n_{\mathrm{H2,out}}S_{\mathrm{H2,out}} + n_{\mathrm{N2,out}}S_{\mathrm{N2,out}} \\ & + n_{\mathrm{NH3,out}}S_{\mathrm{NH3,out}} - n_{\mathrm{H2,in}}S_{\mathrm{H2,in}} - n_{\mathrm{N2,in}}S_{\mathrm{N2,in}} \\ & - n_{\mathrm{He,in}}S_{\mathrm{He,in}} = Q'/T. \qquad [6]\end{aligned}$$

In Eq. [5], ΔH , Q', and P are the change in enthalpy (of the exit minus the inlet) per unit time, the heat input per unit time, and the power produced by the system, respectively. The terms $n_{i,\mathrm{in}}$ and $n_{i,\mathrm{out}}$ are molar flowrates of species i in the inlet feed and reactor exit stream, respectively. The terms $H_{i,\mathrm{in}}$ and $H_{i,\mathrm{out}}$ represent molar enthalpies of species i at the inlet and exit, respectively. Similarly, in Eq. [6], ΔS is the change in entropy per unit time and S_i is the molar entropy of species i. If the inlet and exit composition are

known, Eqs. [5] and [6] can be solved simultaneously and the values of Q' and P can be found. Assuming the mixtures to exhibit ideal gas behavior, and taking into account that $\Delta H_R - T\Delta S_R = \Delta G_R$, (where ΔH_R, ΔS_R, and ΔG_R are the enthalpy, entropy, and free energy change for the reaction of ammonia synthesis), the electrical power P will be given from

$$\begin{aligned} P = &-n_{NH3,out}\Delta G_R - RT\, n_{NH3,out}\ln(Y_{NH3,out}) \\ &+ RT\{n_{H2,in}\ln(Y_{H2,in}) + n_{N2,in}\ln(Y_{H2,in}) \\ &+ n_{He,in}\ln(Y_{He,in})\} - RT\{n_{He,out}\ln(Y_{He,out}) \\ &+ n_{H2,out}\ln(Y_{H2,out}) + n_{N2,out}\ln(Y_{N2,out})\}, \end{aligned} \quad [7]$$

where $Y_{i,in}$ and $Y_{i,out}$ are the inlet and outlet mole fractions of compound i.

Results of calculations for the data of Figs. 5 and 6 are shown in Table 1. The first five columns of the table contain experimental data. The first, second, and third columns contain the H_2/N_2 ratio, the electrical current I, and the total cell potential E_{tot}, respectively. The forth column contains values of P_{exp}, which were calculated from

$$P_{exp} = E_{tot}\cdot I - I^2\cdot R_{ohm}, \quad [8]$$

where R_{ohm} is the ohmic resistance of the electrolyte. The value of R_{ohm} was calculated separately by using the technique of current interruption (22). The fifth column contains the Λ values that were experimentally observed. The sixth and seventh columns contain values that were calculated using Eq. [7]. If the inlet and exit composition are known, Eq. [7] can be solved for P and this value is P_{th}; i.e., it is the minimum electrical power that must be given to the system in order to obtain this exit composition. The sixth column contains these P_{th} values. If $P = P_{exp}$ and the inlet composition is known, Eq. [7] can be solved to determine the outlet. The values of Λ that correspond to that exit composition are shown as Λ_{th}, in the last column of Table 1. Physically, Λ_{th} corresponds to the maximum enhancement that can be obtained, i.e., if all the electrical power P_{exp} is utilized to convert hydrogen and nitrogen into ammonia.

TABLE 1

Theoretical and Experimental Λ's and Electrical Power Requirements

(a) Data of Fig. 5						
P_{H2}/P_{N2}	I (A)	E_{tot} (Volt)	P_{exp} (Watt)	Λ	P_{th} (Watt)	Λ_{th}
3.0	3×10^{-4}	−0.391	-8.1×10^{-5}	0.9	-2.6×10^{-5}	2.2
3.0	6×10^{-4}	−0.780	-3.2×10^{-4}	1.3	-9.7×10^{-5}	3.5
3.0	1.0×10^{-3}	−1.693	-8.4×10^{-4}	1.8	-2.7×10^{-4}	4.7
3.0	1.3×10^{-3}	−1.693	-1.5×10^{-3}	1.8	-3.8×10^{-4}	6.0
3.0	1.6×10^{-3}	−2.050	-2.3×10^{-3}	1.9	-4.9×10^{-4}	6.9
(b) Data of Fig. 6						
P_{H2}/P_{N2}	I (A)	E_{tot} (Volt)	P_{exp} (Watt)	Λ	P_{th} (Watt)	Λ_{th}
1.0	1.0×10^{-3}	−1.735	-1.0×10^{-3}	1.3	-4.5×10^{-5}	4.7
2.6	1.0×10^{-3}	−1.558	-9.6×10^{-4}	1.9	-4.2×10^{-4}	3.4
3.2	1.0×10^{-3}	−1.243	-8.4×10^{-4}	1.8	-2.7×10^{-4}	4.9
4.9	1.0×10^{-3}	−1.196	-1.1×10^{-3}	2.6	-5.9×10^{-4}	6.5

By comparing P with P_{exp} in the table, one can notice that a significant fraction of the electrical energy supplied to the system is converted into chemical energy. This is verified by comparing the values of Λ and Λ_{th}. The Λ_{th} values represent the thermodynamic upper limits of Λ and it can be seen that they are quite low, less than 7.0. Therefore, Λ values of the order of 100 or 1000 could not be observed in these experiments.

The present results indicate that the effect of electrochemical "pumping" of protons is mixed, electrochemical, and catalytic. On one hand, the H^+ flux serves as the carrier of electrical power that is consumed for the synthesis of ammonia at atmospheric pressure. On the other hand, H^+ "pumping" modifies the catalytic properties of the Pd surface and promotes the reaction so that it is not necessary to supply electrochemically all the hydrogen that is stoichiometrically required. To our knowledge, this is the first time that the NEMCA effect is observed in an equilibrium limited catalytic reaction.

Although a lot of additional experiments will be required to come up safely with a reaction scheme, one possible reaction pathway is

$$H_2 \text{ <----> } 2\,H_{ads} \quad [a]$$

$$N_2 \text{ <----> } 2\,N_{ads} \quad [b]$$

$$N_{ads} + H^+ \text{ <----> } NH^+_{ads} \quad [c]$$

$$NH^+_{ads} + e^- \text{ <----> } NH_{ads} \quad [d]$$

$$NH_{ads} + H_{ads} \text{ <----> } NH_{2ads} \quad [e]$$

$$NH_{2ads} + H_{ads} \text{ <----> } NH_{3ads} \quad [f]$$

$$NH_{3ads} \text{ <----> } NH_3 \quad [g]$$

with [c] being a strong candidate for rate determining step. It should be pointed out, however, that the reaction scheme proposed by Rod *et al.* (21), which assumes the reaction to proceed without dissociation of N_2, can explain the experimental observations equally well.

This electrochemical process offers an alternative route that permits operation at desired pressures and temperatures without the thermodynamic restrictions imposed on conventional catalytic reactors. It will take a lot of experimental work plus a thorough technoeconomic analysis and comparison of the present process with the conventional high-pressure process in order to determine if this alternative will become financially preferable.Work toward this goal is currently underway.

ACKNOWLEDGMENTS

We gratefully acknowledge financial support of this research by the Chemical Process Engineering Research Institute (C.P.E.R.I.) of Thessaloniki.

REFERENCES

1. Satterfield, C. N., "Heterogeneous Catalysis in Practice." McGraw–Hill, New York, 1980.
2. Kirk-Othmer, "Encyclopedia of Chemical Technology," forth ed. Wiley, New York, 1986.
3. Ullman's, "Encyclopedia of Industrial Chemistry," Vol. A2, sixth ed., 1988.
4. Boudart, M., *Cat. Rev. Sci. Eng.* **23**, 1 (1981).
5. Temkin, M. I., *Adv. Catal.* **28**, 173 (1979).
6. Emmet, P. H., in "The Physical Basis for Heterogeneous Catalysis" (E. Draughis and R. Jaffee, Eds.). Plenum Press, New York, 1974.
7. Nielsen, A., *Cat. Rev. Sci. Eng.* **23**, 17 (1981).
8. Panagos, E., Voudouris, I., and Stoukides, M., *Chem. Eng. Sci.* **51**, 3175 (1996).
9. Marnellos, G., Sanopoulou, O., Rizou, A., and Stoukides, M., *Solid State Ionics* **97**, 375 (1997).
10. Marnellos, G., and Stoukides, M., *Science* **282**, 98 (1998).
11. Athanasiou, C., Marnellos, G., Tsiakaras, P., and Stoukides, M., *Ionics* **2**, 253 (1996).
12. Bonanos, N., Ellis, B., and Mahmood, M. N., *Solid State Ionics* **28–30**, 579 (1988).
13. Hamakawa, S., Hibino, T., and Iwahara, H., *J. Electrochem. Soc.* **140**, 459 (1993).
14. Chiang, P.-H., Eng, D., and Stoukides, M., *Solid State Ionics* **61**, 99 (1993).
15. Hamakawa, S., Hibino, T., and Iwahara, H., *J. Electrochem. Soc.* **141**, 172 (1994).
16. Stoukides, M., *Cat. Rev.-Sci. Eng.* **42**, 1 (2000).
17. Vayenas, C. G., Jaksic, M. M., Bebelis, S. I., and Neophytides, S. G., The electrochemical activation of catalytic reactions, in "Modern Aspects in Electrochemistry" (Bockris, Conway, and White, Eds.), Vol. 29, p. 57. Plenum, New York, 1996.
18. Vayenas, C. G., Bebelis, S. I., Yentekakis, I. V., and Neophytides, S. N., Electrocatalysis and electrochemical reactors, in "The CRC Handbook of Solid State Electrochemistry" (Gellings and Bouwmeester, Eds.), Chap. 13, pp. 445–480. CRC Press, Boca Raton, FL (1997).
19. Stoukides, M., and Vayenas, C. G., *J. Catal.* **70**, 137 (1981).
20. Pitselis, G. E., Petrolekas, P. D., and Vayenas, C. G., *Ionics* **3**, 110 (1997).
21. Rod, T. H., Logadottir, A., and Norskov, J. K., *J. Phys. Chem.* **112**, 12 (2000).
22. Zisekas, S., and Stoukides, M., in preparation.